COUPLED HEAT TRANSFER IN A COMPOSITE MATERIAL

A. M. Grishin, A. N. Golovanov,
and A. S. Yakimov

UDC 536.24

Numerous studies [1, 2] have been devoted to the mathematical modeling of heat- and mass-transfer processes in composite materials. The thermomechanical disintegration of a composite laminate on the side of a solid of revolution under the influence of a specified heat flux was examined in [1]. In [2], investigators employed a coupled formulation to determine the interaction of a high-enthalpy flow with a hybrid composite composed of a porous solid of revolution and an impermeable cone. However, the mathematical model of heat- and mass-transfer (HMT) in [2] was written without allowance for the flow of heat between the cone and the porous body (Fig. 1). Also, the calculated results in [2] for the porous part of the system were obtained in a one-temperature approximation. At the same time, it is known [3] that, in the general case, the temperatures of the gas and the condensed phase (c-phase) in gas-permeable media are different.

The authors of [4-6] presented an extensive bibliography of studies which have examined the thermal state of porous cooling systems [7-9]. However, as was noted in [4], the results are not comparable – either as a result of appreciable arbitrariness or due to improper formulation of the boundary conditions. In the domestic and foreign literature [4, 7, 9] devoted to mathematical modeling of HMT processes in a two-temperature medium, convective heat transfer is generally ignored in the energy conservation equation for the gas phase when the temperature field is being calculated. At the same time, when the latter was allowed for in [8], it was assumed that all of the heat flowing to the external boundary reached the surface of the skeleton (as it would in the case of a one-temperature medium). In addition, a mild boundary condition $(\partial^2 T_2/\partial n^2)|_{n=0} = 0$) or the condition of thermal insulation) was posited for the gas. Study of the HMT characteristics for two types of gas-permeable media showed [10] that balance (in the sense of conservation laws) boundary conditions are invariant to the thermophysical properties of a two-temperature porous medium. The range of application of mild boundary conditions was established in [10].

The goal of the present study is to use a two-temperature model of a porous inert medium to examine the internal HMT mechanism for a shell composed of different materials. Mathematical experiments show that the following must be done to properly solve the problem: allow for the fact that the porous medium has two temperatures; use materials whose structural characteristics maximize the interphase heat-transfer coefficient; use a cermet as the thermal shield.

1. Formulation of the Problem. To simplify the analysis, we will assume that: the medium has two temperatures, ie. the gas phase and the c-phase have different temperatures; the mass flow along a normal to the surface of the body in the main flow is considerably greater than the mass flow along the generatrix of the surface; the body is not destroyed by its interaction with the gas flow, and no heterogeneous or homogeneous chemical reactions or phase transformations take place on its surface or inside it; the density of the gas phase is determined from the equation of state of an ideal gas; the compositions of the injected gas and the gas in the incoming flow are the same; the heat flux on the heated outside of the conical part of the body is assigned in such a way that the temperature of the surface of the cone by the end of thermal loading ($t = t_0$) is less than the melting point of the given material.

The consumption of the gas-coolant will be determined from simultaneous solution of the continuity equation and the nonlinear Darcy's law [5, 6, 8]. The fact is that high mass velocities $(\rho v)_w$ (Re > 10) are associated with a tubulent filtration regime [6] characterized by a quadratic dependence of the pressure gradient on velocity.

Tomsk. Translated from Zhurnal Prikladnoi Mekhaniki i Tekhnicheskoi Fiziki, No. 4, pp. 141-148, July-August, 1991. Original article submitted February 8, 1990.

 0021-8944/91/3204-0600$12.50

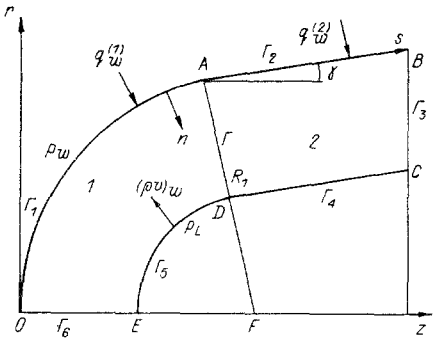

Fig. 1

The mathematical problem of calculating the HMT characteristics in natural coordinates reduces to the solution of the system of conservation equations

$$\partial(\rho_2\varphi v r H)/\partial n = 0; \tag{1.1}$$

$$\rho_1 c_{p1}(1-\varphi)\frac{\partial T_1}{\partial t} = \frac{1}{rH}\left\{\frac{\partial}{\partial n}\left[rH\lambda_1(1-\varphi)\frac{\partial T_1}{\partial n}\right] + \frac{\partial}{\partial s}\left[\frac{r\lambda_1(1-\varphi)}{H}\frac{\partial T_1}{\partial s}\right]\right\} - A_V(T_1 - T_2); \tag{1.2}$$

$$c_{p2}\left(\rho_2\varphi\frac{\partial T_2}{\partial t} + \rho_2\varphi v\frac{\partial T_2}{\partial n}\right) = \left[\frac{\partial}{\partial n}\left(rH\lambda_2\varphi\frac{\partial T_2}{\partial n}\right) + \frac{\partial}{\partial s}\left(\frac{r\lambda_2\varphi}{H}\frac{\partial T_2}{\partial s}\right)\right]\frac{1}{rH} + A_V(T_1 - T_2); \tag{1.3}$$

$$A\mu v + B\rho_2\varphi v|v| = -\partial p/\partial n; \tag{1.4}$$

$$p = \rho_2 R T_2/M, \quad r = (R_1 - n)\sin(s/R_1), \quad H = (R_1 - n)/R_1,$$
$$\mu \sim \sqrt{T_2}, \ \lambda_2 \sim \sqrt{T_2}, \ \varphi = \text{const}; \tag{1.5}$$

$$\rho c_p\frac{\partial T}{\partial t} = \frac{\partial}{\partial n}\left(\lambda\frac{\partial T}{\partial n}\right) + \frac{\partial}{\partial s}\left(\lambda\frac{\partial T}{\partial s}\right) + \frac{\lambda}{r}\left(\frac{\partial T}{\partial s}\sin\gamma - \frac{\partial T}{\partial n}\cos\gamma\right), \tag{1.6}$$
$$r = (R_1 - n)\cos\gamma + (s - s_A)\sin\gamma.$$

System (1.1)-(1.4), (1.6) must be solved with allowance for the following initial and boundary conditions:

$$T_1|_{t=0} = T_2|_{t=0} = T|_{t=0} = T_i; \tag{1.7}$$

on the heated outside surface of the porous tip OA (region I in Fig. 1)

$$\left(q_w^{(1)} - \varepsilon^{(1)}\sigma T_{1w}^4\right)(1-\varphi) = -\lambda_1(1-\varphi)(\partial T_1/\partial n)|_{\Gamma_1}; \tag{1.8}$$

$$\varphi q_w^{(1)} = -\lambda_2\varphi(\partial T_2/\partial n)|_{\Gamma_1}, \quad q_w^{(1)} = \alpha^{(1)}(h_{e0} - c_{p2}T_{1w}); \tag{1.9}$$

on the symmetry axis OE

$$(\partial T_1/\partial s)|_{\Gamma_6} = 0, \quad (\partial T_2/\partial s)|_{\Gamma_6} = 0; \tag{1.10}$$

and on the inside surface of region 1

$$-\lambda_1(1-\varphi)(\partial T_1/\partial n)|_{\Gamma_5} = \delta\left(T_1|_{\Gamma_5} - T_i\right); \tag{1.11}$$

$$T_2|_{\Gamma_5} = \frac{\delta}{c_{p2}(\rho v)_w}\left(T_1|_{\Gamma_5} - T_i\right) + T_i. \tag{1.12}$$

On the line AD between regions 1 and 2, we assign conditions of ideal contact

TABLE 1

T, K	c_{p1}, J/(kg·K)	λ_1, W/(m·K)
300	701,3	0,101
400	950,2	0,11
500	1372	0,115
600	1804	0,125

$$H^{-1}\lambda_1(1-\varphi)\frac{\partial T_1}{\partial s}\Big|_{\Gamma_-} = \lambda\frac{\partial T}{\partial s}\Big|_{\Gamma_+}, \quad T_1|_{\Gamma_-} = T|_{\Gamma_+} = T_2|_{\Gamma_-}; \tag{1.13}$$

and on the solid heated outside surface AB

$$q_w^{(2)} - \varepsilon^{(2)}\sigma T_w^4 = -\lambda\frac{\partial T}{\partial s}\Big|_{\Gamma_2}, \quad q_w^{(2)} = \alpha^{(2)}(h_{e0} - c_{p2}T_w\,. \tag{1.14}$$

On the broken line BCD of region 2, we assign conditions of thermal insulation

$$(\partial T/\partial s)|_{\Gamma_3} = 0, \quad (\partial T/\partial n)_{\Gamma_4} = 0\,. \tag{1.15}$$

On the outside and inside surfaces of region 1, we have equal pressures in the pores and in the surrounding medium:

$$p|_{\Gamma_1} = p_w, \quad p|_{\Gamma_5} = p_L. \tag{1.16}$$

Boundary condition (1.12) is obtained, with allowance for injection [5], from Eq. (1.11) and the balance relation for the temperature at the boundary between the body and the environment

$$(1-\varphi)\lambda_1\frac{\partial T_1}{\partial n}\Big|_{\Gamma_5} + \varphi\lambda_2\frac{\partial T_2}{\partial n}\Big|_{\Gamma_5} = (\rho v)_w\left(h_2^{(1)} - h_i^{(1)}\right) \quad \left(h_2^{(1)} = c_{p2}T_2\right)$$

with the condition $(\varphi\lambda_2\partial T_2/\partial n)|_{\Gamma_5} \ll (1-\varphi)\lambda_1(\partial T_1/\partial n)|_{\Gamma_5}$, $h_i^{(1)} = c_{p2}T_i$. We thus use (1.12) to assign the relative heating of the heat carrier $(T_2|_{\Gamma_5} - T_i)/(T_1|_{\Gamma_5} - T_i)$ until the approach to the inside surface of region 1. This heating is generally determined by the unknown quantity δ.

The heat-transfer coefficient in the expression for convective heat transfer in region 1 is found from the formula [3]

$$\alpha^{(1)} = \xi\eta\exp\left[-0{,}37\,(\rho v)_w/\xi\eta\right], \quad \eta = k_1/R_1^{0,2}(1 + c_{p2}T_{1w}/h_{e0})^{2/3},$$
$$\xi = 3{,}75\sin(s/R_1) - 3{,}5\sin^2(s/R_1). \tag{1.17}$$

In region 2, $\alpha^{(2)} = f(t, s)$ is given by the analytic expression

$$\alpha^{(2)} = 1{,}27s/R_1\exp(s/k_4), \quad 0 \leqslant t < 1\,\text{sec}$$
$$\alpha^{(2)} = k_2[k_3 - \exp(0{,}4t + t/t_0)]s\exp(s/k_1)/R_1, \quad t \geqslant 1\,\text{sec}\,. \tag{1.18}$$

Here t is time; r and z are the transverse and longitudinal components of the cylindrical coordinate system; n and s are the components of the natural coordinate systemn; T is temperature; p is pressure; ρ is true density; v is gas filtration velocity in region 1; $(\rho v)_w$ is the rate of flow of the gas-coolant in the pores; c_p, λ, μ, and δ are the heat capacity, thermal conductivity, absolute viscosity, and coefficient of heat transfer on the inside surface of the shell; φ is porosity; A_V is the bulk coefficient of heat transfer between the gas and the skeleton; R is the universal gas constant; A and B are the viscous and inertial coefficients in Darcy's law; σ is the Stefan-Boltzmann constant; $\varepsilon^{(i)}$ (i = 1, 2) is the emissivity of the surface of the skeleton and graphite; R_1 is the external radius of the blunting of the body; L_{OE} is the thickness of the shell; s_{OB} is the length of the body along the generatrix; $\alpha^{(i)}$ is the heat-transfer coefficient in the

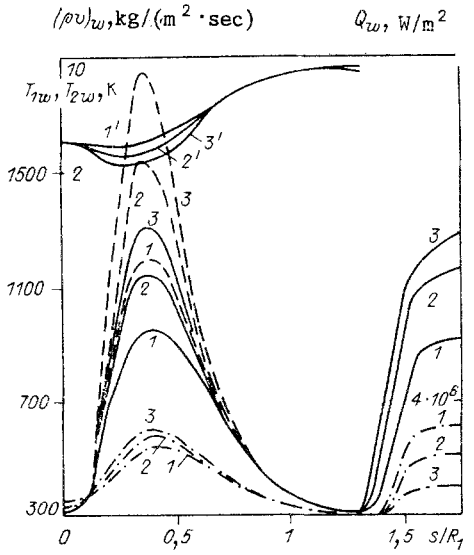

Fig. 2

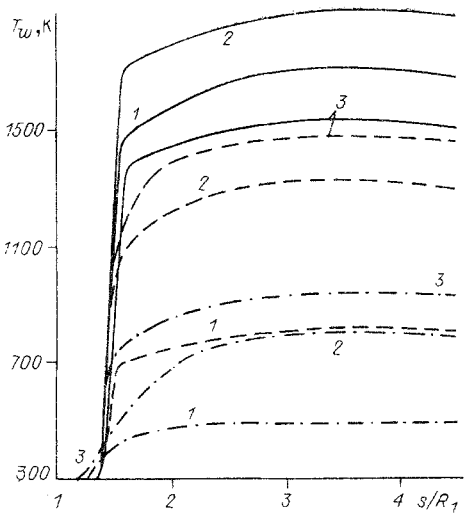

Fig. 3

formula for convective heat flux; γ is the cone angle; $q_w^{(i)}$ (i = 1, 2) is the convective heat flux from the gas phase; $Q_{w1} = (q_w^{(1)} - \varepsilon^{(1)}\sigma T_{1w}^4)(1 - \varphi)$, $Q_{w2} = q_w^{(2)} - \varepsilon^{(2)}\varphi T_w^4$ is the total heat flux to the c-phase on the sphere and on the cone, respectively; h is enthalpy; M is the molecular weight of air; Nu, Pe, and Re are the Nusselt, Peclet, and Reynolds numbers; the indices e and e0 are affixed to quantities on the external boundary of the boundary layer and at the stagnation point, respectively; w and L are indices denoting thermodynamic parameters on the external and internal boundaries of the gaseous and c-phases; superscripts 1 and 2 denote parameters in regions 1 and 2, while subscripts 1 and 2 denote the skeleton and the gas in region 1; the subscript i denotes initial values; V denotes bulk values; 0 denotes the end of thermal loading; * denotes characteristic quantities.

2. Method of Calculation, Initial Data. The pressure on the heated outside surface of the body $p_w = p_* p_{e0}$ was found from formulas for spheres [11]: $p_* = 1 - 1.17\sin^2(s/R_1) + 0.225\sin^6(s/R_1)$, while a constant pressure was assigned for the stagnation point. The pressure on the "cold" inside surface of the shell of the sphere was taken in the form $p_L = 1.2p_{e0}$, which was sufficient to ensure the necessary coolant flow rate on the thermally loaded section from t = 0 to $t = t_0$.

The quasisteady continuity equation $\rho_2\varphi v = -(\rho v)_w r_w/rH$ (the minus sign is due to the fact that the normal component of the coordinate n is directed into the body (see Fig. 1), while the coolant flows in the opposite direction) can be integrated along with Eq. (1.5), nonlinear Darcy's law (1.4), and boundary condition (1.16), and we can find gas velocity and pressure across the layer in region 1:

$$(\rho v)_w(s) = \{[2B(p_L^2 - p_w^2)\varphi M D_L/R + E_L^2]^{0.5} - E_L\}/2BD_L; \tag{2.1}$$

$$p(s, n) = \{p_w^2 + 2R[B(\rho v)_w^2 D + (\rho v)_w E]/M\}^{0.5}, \tag{2.2}$$

where

$$D(s, n) = \int_0^n T_2 (r_w/rH)^2\, dn; \quad E(s, n) = A\int_0^n \mu T_2 (r_w/rH)\, dn.$$

Boundary-value problem (1.2)-(1.3), (1.6)-(1.15) was solved numerically by means of the locally unidimensional splitting method [12]. We used implicit, monotonic, absolutely stable difference schemes with a total approximation error $O(\tau + H_{1i+1} - H_{1i} + H_{2j+1} - H_{2j})$ (H_{1i} is the variable space step along the coordinate s, while H_{2j} is the same along the coordinate n). Here, we automatically chose the time step τ on the basis of the specified accuracy condition and the convergence of the iterations with respect to T_1 and T_2. If the maximum time step is no greater than 0.5, then obtaining a solution on a BÉSM-6 computer

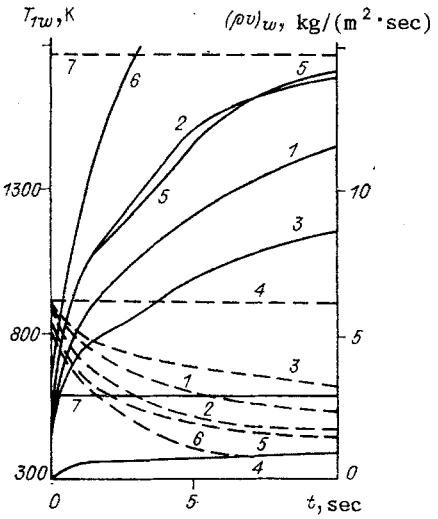

Fig. 4

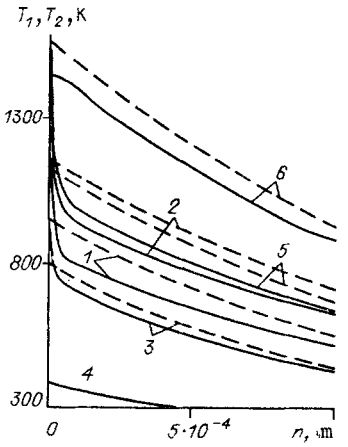

Fig. 5

takes 5 min for T_1 (31 × 17) and T_2 (21 × 17). The numerical program was also tested against the exact analytical solution [13]. The deviation of the former from the latter on the given time interval was no greater than 0.76%. The integral in Eq. (2.2) was found from the trapezoid formula. In obtaining the numerical solution, it was necessary to condense the difference grid with respect to the space coordinate n near the heated boundary in order to avoid computing difficulties connected with the small parameter accompanying the highest derivative in Eq. (1.3).

The thermophysical and structural characteristics of the porous material were taken from [14] for a specimen made of sintered powdered stainless steel. Here, T_i = 300 K, $h_{e0} = 6.1\cdot10^6$ J/kg, $\lambda_1 = 2.92 + 4.5\cdot10^{-3}T_1$ W/(m·K), $\rho_1 c_{p1} = (1252 + 0.544T_1) \times 10^3$ J/(m^3·K), φ = 0.34, $L_{OE} = 4\cdot10^{-3}$ m, $s_{OB} = 0.2725$ m, $\varepsilon^{(1)} = 0.7$, $c_{p2} = 10^3$ J/(m^3·K), Δ = 100 W/(m^2·K), $A = 2.3\cdot10^{11}$ m^{-2}, $B = 5.7\cdot10^5$ m^{-1}, R = 8.31 J/(mole·K), $\gamma = 10^\circ$, $R_1 = 5\cdot10^{-2}$ m, $\sigma = 5{,}7\cdot10^{-8}$ W/(m^2·K^4), $p_{e0} = 4.10^5$ N/m^2, $t_0 = 10$ sec, $k_1 = 1.76$, $k_2 = 0.7$, $k_3 = 2.5$, $k_4 = 0.18$.

The characteristic values at $T_* = 10^3$ K in the formula for the viscosity and thermal conductivity of air ($\lambda_2 = \lambda_* \sqrt{T_2/T^*}$, $\mu = \mu_* \sqrt{T_2/T_*}$) were taken from [15]: M = 0.029 kg/mole, $\mu_* = 4.2\cdot10^{-5}$ kg/(m·sec), $\lambda^* = 6.7 \times 10^{-2}$ W/(m·K). The thermophysical parameters and emissivity of VPP graphite were taken from [16].

The thermophysical characteristics of porous cermet $Al_2O_3$40% + $Si_3N_4$60 % with φ = 0.36, were determined using IT-c_p-400 and IT-λ-400 units to measure heat capacity and thermal conductivity [17]. The effective values of these quantities in relation to temperature are shown in Table 1. The total statistical errors of the parameters are no greater than 6.9 and 7.7%, respectively, while the density of the porous ceramic is 2072.8 kg/m^3. Filtration characteristics A and B in nonlinear Darcy's law (1.4) were obtained by the method in [18]: $A = (1.6 \pm 0.2)\cdot10^{10}$ m^{-2}, $B = (6.56 \pm 0.1)\cdot10^3$ m^{-1}. The value of $Re = (\rho v)_w \ell_* \mu_*/\mu$ was varied within the range 1.57-2.37. Since B is small, we used the quantity $\ell_* = \sqrt{A^{-1}}$ as the characteristic dimension in the Reynolds number.

An analysis of the literature data shows [3, 5, 6, 14, 19] that despite the large number of studies devoted to heat transfer in porous media, there is a sizable difference in the heat-transfer coefficients A_V. Experimental data on intrapore heat transfer was generalized in [19] using the simularity equation

$$Nu_V = 0.015Pe^{n_1}, \quad n_1 = 1 - 1.3, \quad 0.5 < Pe < 80. \tag{2.3}$$

The quantity $\ell_* = B/A$ was used in [19] in analyses performed on the basis of (2.3). Here, B and A are determined empirically for the given specimen. This approach makes it possible to account for the relationship between hydraulic resistance and heat transfer in the function $Nu_V = f(Pe)$. The use of criterional relation (2.3) for a porous ceramic with $n_1 = 1.3$ gives $A_V = 1.1\cdot10^7$ W/(m^3·K), while for porous steel [14] $A_V = 3.6\cdot10^7$ W/(m^3·K).

Let isothermal heating of the cermet take place with assigned pressures $p_L = 1.25\cdot10^5$ N/m^2 and $p_w = 10^5$ N/m^2. Then with known A and B and T = 300 K, without allowing for the geometry of the shell we can use Eq. (2.1) to find the flow rate $(\rho v)_w = 5.03$ kg/(m^2·sec).

An experiment conducted with these heating conditions yields $(\rho v)_w = 5.48$ kg/(m^2·sec), which is no greater than 8%.

3. Analysis of the Results of the Numerical Solution. First let us examine the first shell heating regime, when the leading part of the shell is made of a porous material [14] and the conical part is made of stainless steel [6]. Figure 2 shows relations for the temperature of the surface of the skeleton T_{1w} and the gas T_{2w} and the total heat flux to the c-phase Q_{wi}, i = 1, 2 (solid, dashed, and dot-dash curves, respectively) at the moments of time t = 2, 4, and 6 sec for an interphase heat-transfer coefficient $A_v = 3.6 \cdot 10^7$ W/(m^3·K). Curves 1′-3′ correspond to the coolant flow rate $(\rho v)_w$ at the same moments of time. It is apparent that an increase in Q_{w1} is accompanied by an increase in the temperature of the skeleton and the gas in the permeable tip. Meanwhile, the maximum tip temperature $T_{1*} = T_{1w}(s_*, t)$ and Q_{w*} are in agreement with the maximum for $\alpha^{(1)}$ in Eq. (1.17). It turns out that the specimen does not fail at the assigned value $A_v = 3.6 \cdot 10^7$ W/(m^3·K) and the pressure $p_L = 1.2 p_{e0}$, since the value $T_{1*} = 1445$ K at $t = t_0$ remains lower than the melting point of the porous steel ($T_{mt} = 1600$ K). The rate of flow of the gas-coolant (see Fig. 2) decreases along the surface on certain sections where gas temperature increases, due to the increased effect of inertial forces compared to pressure in Darcy's law (1.4).

The temperature of the surface T_w of the conical part of the shell for materials based on a ceramic [20], steel [6], and VPP graphite [16] (solid, dashed, and dot-dash lines) is shown in Fig. 3 for the moments of time t = 1, 4, 8 sec (lines 1-3). Since the diffusivity of the ceramic is an order lower than the diffusivity of the steel – which is in turn an order lower than the diffusivity of the graphite – then the depth to which the materials are heated and the temperature of their surfaces decrease and increase, respectively, in the same order. Since the thermal conductivity of graphite and steel are of the same order, the heating of the porous body over a depth of one interval of s from the joint to the cone was 338 and 351 K at $t = t_0$, respectively, while heat conduction amounted only to 305 K for the ceramic due to its low thermal conductivity. It is apparent that the good heat-insulating properties of the last-named material make it suitable for use as a structural element in heat shields.

Other conditions being equal, a change in the boundary conditions for δ to 500 produces neither a qualitative nor a quantitative change in the solution of the problem.

Solid lines 1-4 in Fig. 4 show profiles of the temperature of the surface of the skeleton T_{1*} corresponding to $A_v = 3.6 \cdot 10^7$, $1.8 \cdot 10^7$, $7.2 \cdot 10^7$, 10^{10} W/(m^3·K) in relation to time (the dashed curves represent the profile $(\rho v)_w$). The dashed and solid curves in Fig. 5 respectively show the distribution of the temperature of the skeleton and the gas depthwise in the section $s = s_*$ at t = 2 sec for the indicated HMT regimes. An analysis of Figs. 4 and 5 shows that a decrease in the rate of heat transfer between the gas and the skeleton ($A_v = 1.8 \cdot 10^7$ W/(m^3·K)) leads to an increase in T_1 and T_2 near the surface of the tip. The fact is that the larger value of T_2 at $A_v = 1.8 \cdot 10^7$ W/(m^3·K) compared to $A_v = 3.6 \cdot 10^7$ W/(m^3·K) leads to a decrease in coolant flow rate (compare curve 2 in Fig. 4), in accordance with Eq. (2.1). Thus, coolant with a higher temperature has less of a cooling effect on the permeable shell. This conclusion, consistent with the results in [7-9], leads to an increase in the heat-transfer coefficient $\alpha^{(1)}$ from (1.17), and it ultimately leads to an increase in convective heat flux $q_w^{(1)}$.

The opposite effect is seen at $A_v = 7.2 \cdot 10^7$ W/(m^3·K) (curves 3 in Figs. 4 and 5). The value $A_v = 10^{10}$ W/(m^3·K) equalizes the temperature of the gas phase and the c-phase (curve 4 in Fig. 5), and it ultimately lowers the temperature of the skeleton surface by 800 K. For a thicker shell ($L = 5 \cdot 10^{-3}$ m and $A_v = 3.6 \cdot 10^7$ W/(m^3·K) – curves 5 in Fig. 4 and 5), a decrease in pressure gradient brings a 33% reduction in coolant flow rate. This in turn leads to an increase in $q_w^{(1)}$ and to destruction of the skeleton for $t = t_0$.

It is necessary to say that for some HMT regimes for the balance boundary conditions (1.8), (1.9) $T_{2w} > T_{1w}$ (Fig. 5, curves 1-3, 5). However, T_1 becomes greater than T_2 with increasing depth. This has to do with the fact that gas flow rate is small for such HMT regimes at t = 2 sec (see Fig. 4). As a result, air temperature increases sharply both on the surface and in a certain region around it due to heat exchange with the environment and the skeleton and the fact that the diffusivity of air is greater than that of the skeleton (steel). Then, as the heat-transfer process becomes established, the c-phase is heated more rapidly – since the thermal conductivity of the porous steel is two orders greater than the thermal conductivity of the gas.

Curves 6 in Figs. 4 and 5 correspond to the regime $A_v = 3.6 \cdot 10^7$ W/(m^3·K) and the condition of thermal insulation for the gas $(\partial T_2/\partial n)|_{r_1} = 0$. In this case, in accordance with

the boundary condition for T_{1w} (1.8), all of the convective heat flux $q_w^{(1)}$ falls on the surface of the skeleton. Since $\varphi = 0.34$, the surface of the c-phase is always heated at a rate which is 30% greater, and it reaches T_{mt} at $t > 2$ sec.

In the case of low porosity ($\varphi = 0.05$), balance boundary conditions (1.8)-(1.9) nearly coincide with the conditions $(\partial T_2/\partial n)|_{r_1} = 0$ [8], since in this case $(\lambda_2\varphi\partial T_2/\partial n)|_{r_1}/[\lambda_1(1-\varphi)\partial T_1/\partial n]|_{r_1} \ll 1$ and all of the heat flux from the gas phase reaches the surface of the framework. Thus, the condition $(\partial T_2/\partial n)|_{r_1} = 0$ can have physical significance only at $\varphi < 0.1$. However, little use is made of low-porosity composites in heat engineering [6]. In addition, it was shown in [10] that the heat-insulation conditions for the gas are not invariant to the thermophysical properties of the two-temperature gas-permeable medium.

Let us now examine a second composite heating regime in which the leading part of the body is a porous ceramic and the conical part is impermeable steel (curves 7 in Fig. 4). In this regime, with $p_{e0} = 1.8\cdot10^5$ N/m^2, $A = 1.6\cdot10^{10}$ m^{-2}, $B = 6.56\cdot10^3$ m^{-1}, $A_v = 1.1\cdot10^7$ W/(m$^3\cdot$K), $L_{OE} = 5.9\cdot10^{-3}$ m, inertial forces and viscosity are small compared to the pressure gradient. The latter quantity also ultimately determines the flow rate of the coolant gas in the porous ceramic (see dashed line 7 in Fig. 4 for $(\rho v)_w$). As a result, the temperature of the gas-coolant increases slightly (to 325 K), while the temperature of the surface of the c-phase reaches steady-state values in tenths of a second (solid line in Fig. 4). Due to the low thermal conductivity of the skeleton (see Table 1) and the high gas velocity, the temperature of the porous part in the region of the joint with the cone remains at the initial value up to $t = t_0$. This fact results in a substantial flow of heat from the conical part of the shell. Thus, at the moment $t = t_0$, the temperature of the surface of the cone about its cirumference is 200-300 K lower than in the first heating regime (in which the leading part is made of porous steel).

The values of T_{1w} and T_{2w} depend to a significant extent on the bulk heat-transfer coefficient A_v. To ensure a reduction in the surface temperature of porous bodies, it is necessary to use materials having structural characteristics that will maximize the value of A_v.

The results of our numerical experiment showed the following: 1) it is necessary to allow for the effect of two temperatures when mathematically modeling heat and mass transfer in porous steel and permeable cermets, since assuming that the porous medium has only one temperature ($A_v \to \infty$) significantly lowers the temperature of the skeleton; 2) it is best to use a material based on a cermet for the heat shield, since, other conditions being equal, there is almost no depthwise heating of the specimen due to the low thermal conductivity of the ceramic.

LITERATURE CITED

1. V. I. Zinchenko and A. S. Yakimov, "Regimes of thermomechanical failure of a composite under the influence of a heat flow," Fiz. Goreniya Vzryva, No. 2 (1988).
2. V. I. Zinchenko, O. P. Fedorova, and A. S. Yakimov, "Calculation of characteristics of coupled heat and mass transfer in the presence of thermomechanical disintegration," Heat and Mass Transfer - MMF, Institute of Heat and Mass Transfer, Academy of Sciences of the Belorussian SSR, Minsk (1988), Sec. 3.
3. Yu. V. Polezhaev and F. B. Yurevich, Thermal Protection [in Russian], Énergiya, Moscow (1976).
4. V. A. Maiorov, "Boundary conditions for a system of intensive transpirational cooling," Inzh.-Fiz. Zh., 47, No. 4 (1984).
5. V. M. Polyaev, V. A. Maiorov, and L. L. Vasil'ev, Hydrodynamics and Heat Transfer in Porous Structural Elements of Aircraft [in Russian], Mashinostroenie, Moscow (1988).
6. R. A. Andrievskii, Porous Cermets [in Russian], Metallurgiya, Moscow (1964).
7. J. Koch and R. Colony, "Analysis of cooling efficiency for the case of coolant flow in a channel with a porous material," Trans. ASME, Ser. C, No. 3 (1974).
8. H. Khubota, "Thermal characteristics of an evaporative cooling system under the combined influence of radiant and convective heating," ibid., No. 4 (1977).
9. V. L. Dorot and M. Kh. Strelets, "Porous cooling in a supersonic turbulent boundary layer," Teplofiz. Vys. Temp., 11, No. 6 (1973).
10. A. M. Grishin, V. I. Laeva, and A. S. Yakimov, "Boundary conditions for a mathematical model of heat and mass transfer in a two-temperature porous medium with a gas flow," Inzh.-Fiz. Zh., 56, No. 6, (1989); Dep. VINITI 02.01.89, No. 21-V89.

11. V. V. Lunev, V. G. Pavlov, and S. P. Sinchenko, "Hypersonic flow of equilibrium dissociating air about a sphere," Zh. Vychisl. Mat. Mat. Fiz., 6, No. 1 (1966).
12. A. A. Samarskii, Theory of Difference Schemes [in Russian], Nauka, Moscow (1977).
13. A. S. Yakimov, "Branching method," ChMMSS, 16, No. 2 (1985).
14. O. M. Alifanov, A. P. Tryanin, and A. L. Lozhkin, "Experimental study of a method of determining the internal heat-transfer coefficient from the solution of the inverse problem," Inzh.-Fiz. Zh., 52, No. 3 (1987).
15. N. B. Vargaftik, Handbook of the Thermophysial Properties of Gases and Liquids [in Russian], FM, Moscow (1963).
16. V. P. Sosedov, Properties of Carbon-Based Structural Materials: Handbook [in Russian], Metallurgiya, Moscow (1975).
17. E. S. Platunov, S. E. Buravoi, V. V. Kurepin, et al., Thermophysical Measurements and Instruments [in Russian], Mashinostroenie, Leningrad (1986).
18. A. P. Kurshin, "Calculation of the hydrodynamic characteristics of a cermet," Tr. TsAGI, No. 1677 (1975).
19. V. F. Zanemonets and V. I. Rodionov, "Experimental study of heat transfer in a particulate composite," Heat and Mass Transfer - MMF, Institute of Heat and Mass Transfer, Academy of Sciences of the Belorussian SSR, Minsk (1988), Sec. 7.
20. V. I. Daukins, K. A. Kazakyavichyus, G. A. Prantskyavichyus, and V. L. Yurenas, Investigation of the Thermal Stability of a Refractory Ceramic [in Russian], Mintis, Vil'nyus (1971).

REFLECTION OF A SHOCK WAVE FROM THE FREE SURFACE OF AN ELASTOPLASTIC BODY

V. A. Baskakov and A. V. Bobryashov

UDC 539.3:534.1

The present article examines a model of a macroscopically isotropic ideal elastoplastic body with small trains within the framework of the classical dynamic theory of plasticity. The behavior of the body is described by the Prandtl-Reuss equations, the von Mises plasticity condition, and the associated flow law [1].

Our goal is to theoretically study a two-dimensional model problem concerning the propagation and reflection of a shock wave of finite length from a free boundary. The time of impact (contact time) is considered to be finite in regard to the generation of the wave. This time reaches ~10^{-6} sec for a broad range of metals, so that the length of the wave may be several millimeters - in which case it must be taken into account. Here, we will examine weak shock waves, the pressure at the front being of the order of 1 GPa. The waves do not produce phase changes in the substance.

Thus, we will be examining questions relating to a single local reflection of loading and unloading waves - a case corresponding to the actual shock loading of a body. Problems that were similarly formulated and were solved by similar approaches were addressed in [2-5].

Shock-wave profiles in metals have been well studied both theoretically and experimentally [6, 7] and constitute an elastic precursor which is followed by a slower-moving plastic front. The shock wave splits in two, with the formation of a two-front wave configuration. Here, in actual physical processes involving high-speed impact, the amplitude (intensity) of the shock wave initially rapidly increases. It then decreases monotonically to zero - which corresponds to unloading. This circumstance makes it very difficult to construct the unloading wave [8]. As a result, we will henceforth assume that unloading occurs in the form of a certain stepped wave which moves with the speed of the precursor.

Since the stresses and displacement rates change sign in the unloading wave (to tension), we can say that the front of this wave, having "caught up with" the front of the

Voronezh. Translated from Zhurnal Prikladnoi Mekhaniki i Tekhnicheskoi Fiziki, No. 4, pp. 148-157, July-August, 1991. Original article submitted January 5, 1990.